Volume 14
Number 3
22 January 2026
Pages 875–1278

Journal of Materials Chemistry C

Materials for optical, magnetic and electronic devices

rsc.li/materials-c

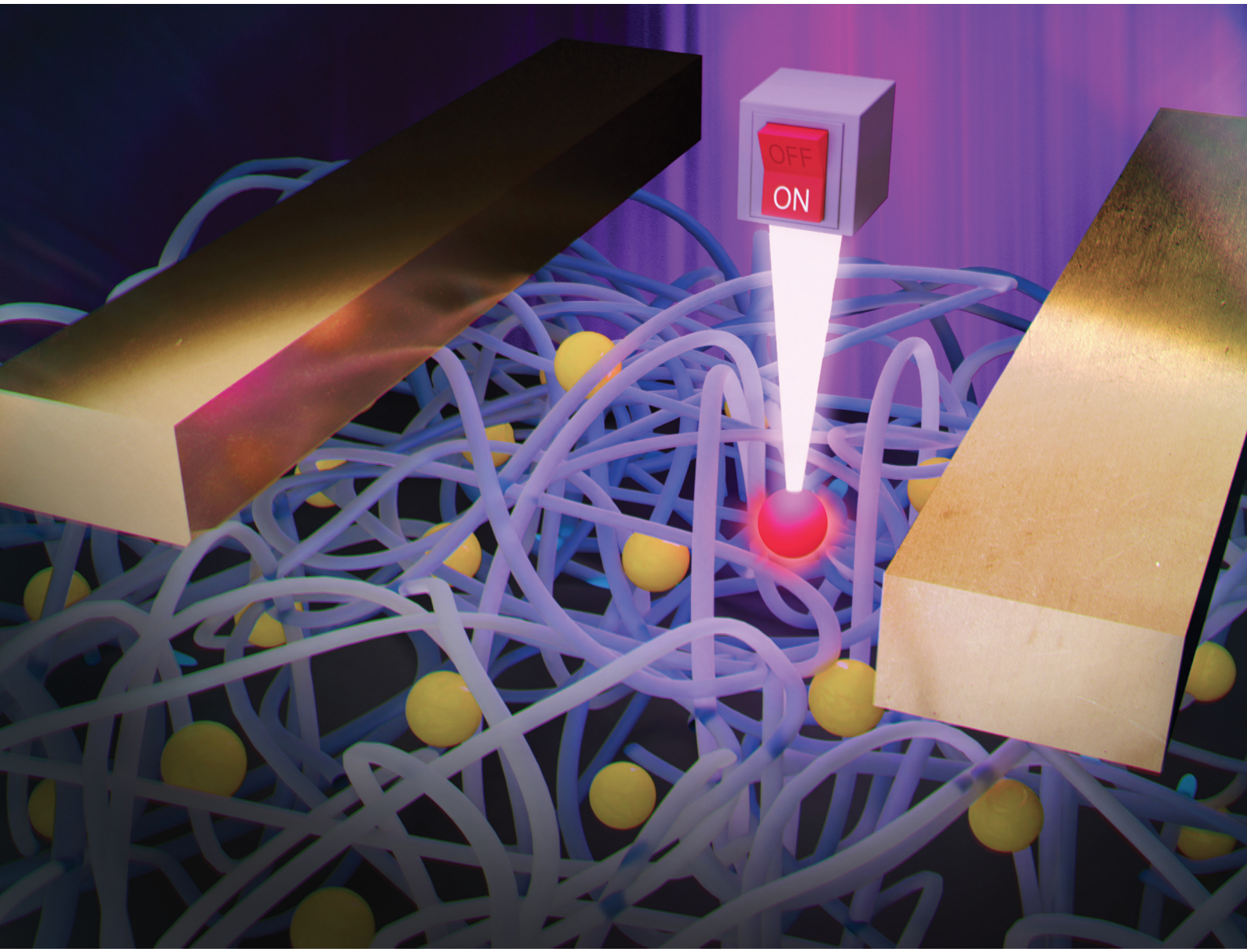

ISSN 2050-7526

ROYAL SOCIETY OF CHEMISTRY

PAPER

Ulrike Kraft *et al.*

Reversible switching through irradiation of capacitors and organic transistors employing dielectrics blended with non-ionic molecular photoswitches

Journal of Materials Chemistry C

ROYAL SOCIETY OF CHEMISTRY

PAPER

View Article Online
View Journal | View Issue

Cite this: J. Mater. Chem. C, 2026, 14, 1027

Reversible switching through irradiation of capacitors and organic transistors employing dielectrics blended with non-ionic molecular photoswitches

Sten Gebel,[a] Oumaima Aiboudi,[b] Parham Derakhshanfar,[a] Jihyun Shin,[a] Ulrike Langklotz,[c] Franziska Lissel[bd] and Ulrike Kraft *[a]

One promising approach to introduce additional functionalities for sensing and memory applications into conventional organic electronic devices is the introduction of stimuli responsive additives, such as molecular switches. These small organic molecules undergo reversible isomerization between (at least) two isomers when irradiated with light of different wavelength resulting in drastic changes in physico-chemical properties such as frontier orbital energy levels, dipole moment and/or molecular geometry. These reversible changes in molecular properties can be exploited to deliberately modify charge transport in organic field-effect transistors and therefore enable optical control over device characteristics. Here, stimuli-responsiveness of organic transistors is achieved by incorporating the dihydroazulene/vinylheptafulvene (DHA/VHF) molecular switches into the gate dielectric. To systematically explore this novel approach, we firstly provide a detailed evaluation of the dielectric properties of the DHA/VHF blends with the dielectric polymer poly(methyl methacrylate) in metal–insulator–metal capacitors using impedance spectroscopy. Afterwards, these switchable dielectric blends are employed as gate dielectrics in OFETs, allowing optical control over device characteristics and figures of merit such as field-effect mobility and threshold voltage. Furthermore, optical absorption spectroscopy shows that DHA/VHF molecular switches (unlike the well-known spiropyran/merocyanine photoswitch) exhibit excellent resistance to cycling fatigue when incorporated into insulating PMMA matrices.

Received 25th April 2025,
Accepted 23rd October 2025

DOI: 10.1039/d5tc01677k

rsc.li/materials-c

Introduction

The increasing demand for mobile and flexible electronics and the rising interest in the "Internet of Things" promotes research on lightweight organic electronic devices and concepts where the integration of silicon chips is too expensive. Organic field-effect transistors (OFETs) can be used as fundamental building blocks for more advanced electronic circuits and applications on flexible foil and paper substrates,[1] such as multi-level photomemories, photodetectors and neuromorphic electronics.[2–4]

Here, we give a detailed account of reversible switching of poly(methyl methacrylate) (PMMA) blends with dihydroazulene/vinylheptafulvene (DHA/VHF) photo-/thermochromic molecules. These molecular switches are promising candidates for enabling novel light-responsive organic electronic devices, since they exhibit a large change in dipole moment, but do not contain any ionic moiety which are known to be detrimental for efficient charge carrier transport. For the spiropyran (SP)/merocyanine (MC) switch for example, the zwitterionic merocyanine has been reported to act as scattering site in functionalized transistors.[5–7] Furthermore, transistors with PMMA:SP/MC gate dielectrics have been reported to be only optically responsive in the bottom-gate configuration, while top-gate transistors are optically inactive due to phase separation,[6] leading to reduced applicability of the system.

So far DHA/VHF switches only received little attention in the context of stimuli-responsive organic devices and previous reports focused mostly on single-molecule junctions or devices based on self-assembled monolayers.[8–11] In this work we functionalize PMMA gate dielectrics with DHA/VHF switches to enable light-programmable top-gate organic transistors. The absence of any ionic moieties in both isomers of the DHA/VHF switches allows, to solely study the effect of the change in dipole moment of the switch (~6–10 D for DHA derivative *versus* ~10–15 D for VHF derivatives) on the dielectric

[a] Organic Bioelectronics Research Group, Max Planck Institute for Polymer Research, Mainz, Germany. E-mail: kraftu@mpip-mainz.mpg.de
[b] Leibniz Institute for Polymer Research, Dresden, Germany
[c] Fraunhofer Institute for Ceramic Technologies and Systems IKTS, Dresden, Germany
[d] Hamburg University of Technology, Hamburg, Germany

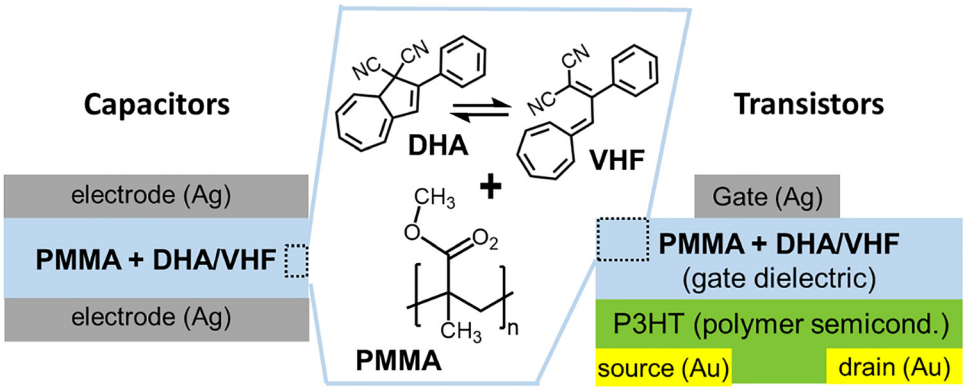

Fig. 1 Schematic illustration of capacitors (MIM, metal–insulator–metal devices) and bottom-contact top-gate polymer transistors with gate dielectrics based on PMMA blends with DHA/VHF photo-/thermochromic molecules and the molecular structures of PMMA, DHA and VHF.

properties of PMMA:DHA/VHF capacitors (MIM, metal–insulator–metal devices) and the device performance of organic transistors. (A schematic illustration is depicted in Fig. 1.)

The gate dielectric is able to dramatically influence morphology, energetic disorder or trapping at the semiconductor/dielectric interface and therefore charge transport and device performance.[12] In this context, the dielectric permittivity ε_r is a key material property. High permittivities for example are generally required for low voltage operation,[13–15] but can also induce energetic disorder and hence lower carrier mobilities.[16,17] Impedance spectroscopy is a commonly-used method to study dielectric properties of insulating polymers and several examples can be found in the literature where it was used to study the effect of small molecule additives such as azo dyes or other organic chromophores within a dielectric matrix.[18–20] Here, we apply impedance spectroscopy in a different context to investigate the photoisomerization of photochromic molecules (also called photoswitches). Photoswitches are molecules that undergo reversible isomerization between (at least) two isomers due to irradiation with light of different wavelengths. Both isomers can exhibit differences in physicochemical properties such as π-conjugation, molecular geometry and/or dipole moment. When switching from DHA to VHF, the increase in the dipole moment will lead to an increase in permittivity and hence to an increase of the capacitance of PMMA:DHA/VHF blends. When applied as gate dielectrics in transistors an increase in capacitance is expected to be reflected in higher drain currents.

As the dipole moments of the two isomers differ significantly, impedance spectroscopy on PMMA:DHA/VHF MIM capacitors will be a valuable tool to investigate the photoswitching and its effect on the dielectric properties of the insulating matrix. The reversible switching of the overall capacitance due to isomerization of photoswitches has been reported by several groups, *e.g. via* blending azobenzene-based photoswitches into PMMA[21] or *via* synthesizing spiropyran-containing dielectric copolymers.[22] However, detailed characterizations of impedance data, frequency-dependence and how the light-induced isomerization of photoswitches *e.g.* affects dielectric permittivity ε_r' and dielectric loss ε_r'' of light-responsive insulating blends are scarce.[23] These kinds of data could not only give further insights into underlying mechanisms, but also allow to quantify the switching capability of photochromic molecules.

In this study, it is shown that the stimulus-induced isomerization of the dihydroazulene/vinylheptafulvene (DHA/VHF) photoswitches within a PMMA matrix can be directly observed by measuring the frequency-dependent complex electrical impedance Z^*. From the impedance spectra the switching parameters such as the complex dielectric permittivity ε_r^* and the area-normalized capacitance of the gate dielectric are derived. An alternative approach to analyzing impedance data is the fitting with an equivalent circuit. This method is widely used in many fields such as electroceramics,[24] battery research[25] or biosensing.[26] However, to the best of our knowledge there is no systematic study implementing and assessing an equivalent circuit model for light switchable organic capacitor devices. Here, an equivalent circuit fitting methodology is employed serving as alternate approach to evaluate the switching capabilities of the DHA/VHF molecules in functioning electronic devices. Furthermore, it is demonstrated for the first time that PMMA:DHA/VHF blend gate dielectrics in organic transistors enable the control of transistor characteristics and figures of merit, by applying external stimuli such as UV light and heat. Additionally, it is shown that DHA/VHF molecular switches (unlike the established SP/MC photoswitch) exhibit excellent resistance to cycling fatigue when incorporated into a PMMA dielectric.

Experimental details

Materials and solution preparation

The molecular switches DHA-Ph, DHA-OMe and DHA-F_2 were synthesized as previously described[27] (see Fig. S1 for molecular structure of the photoisomers for the three photoswitches). PMMA (product number 200 336, average molecular weight = 15 kDa, PDI: 1.83) and regioregular P3HT (poly(3-hexylthiophen, product number 445 703, molecular weight = ~50 kDa, regioregularity >90%, further information is provided in the SI, section S9) were purchased from Sigma Aldrich and used without further purification. PMMA stock solutions were

prepared with anhydrous trichloromethane (80 mg mL^{-1}, for capacitor and UV/Vis absorption spectroscopy experiments) or anhydrous ethyl acetate (120 mg mL^{-1}, for transistor experiments). For the photoswitch stock solutions, the solvent was chosen to match the solvent of PMMA (35 to 40 mg mL^{-1} in anhydrous trichloromethane or 52 to 60 mg mL^{-1} in anhydrous ethyl acetate). PMMA and switch solutions were prepared in air and stirred over night at room temperature, while P3HT solutions (10 mg mL^{-1} in anhydrous chlorobenzene) were prepared in a nitrogen-filled glovebox and stirred over night at 60 °C. The final PMMA solutions (40 mg mL^{-1} in anhydrous trichloromethane or 60 mg mL^{-1} (80 mg mL^{-1} for PMMA-only reference) in anhydrous ethyl acetate) were prepared by adding either switch stock solution or additional solvent (for reference devices) to the PMMA stock solution and were stirred for 2 h at room temperature prior to spin coating. The molar fractions of photoswitch (with respect to a single PMMA repeat unit) in these solutions was 14.6 mol% (*i.e.* 14.6 switch molecules in proportion to 100 PMMA repeat units), resulting in the following mass fractions: 30.44 wt% (DHA-Ph), 32.89 wt% (DHA-OMe) and 33.33 wt% (DHA-F_2).

Device fabrication and UV/temperature treatments

Capacitors (metal–insulator–metal structures[28]) and bottom-contact/top-gate transistors were fabricated on glass substrates. Prior to bottom electrode deposition, the substrates were cleaned *via* sonicating in ultrapure water (5 min), acetone and isopropanol (both 10 min). After drying the substrates in an oven (10 min at 140 °C) a UV/ozone treatment was applied for 20 min. Capacitor bottom electrodes (5 nm chromium/100 nm silver) and transistor source and drain electrodes (2 nm chromium/30 nm gold, channel length = 30 μm, channel width = 1 mm) were thermally evaporated in vacuum ($<1 \times 10^{-7}$ mbar) through shadow masks. The glass substrates for transistors were exposed to 20 min UV/ozone treatment prior to deposition of the organic semiconductor layer. P3HT films (thickness = 30–35 nm) were fabricated *via* spin coating at 1500 rpm for 30 s and annealed for 30 min at 150 °C. PMMA:photoswitch blends or bare PMMA dielectrics were spin coated either on top of the bottom electrode (capacitors) or the P3HT film (OFETs) at 2000 rpm for 60 s to yield films with a thickness of 600–650 nm/710–730 nm (trichloromethane/ethyl acetate) for films containing PMMA:photswitch blends and 400–460 nm/700–720 nm (trichloromethane/ethyl acetate) for bare PMMA films. (Thickness profiles are shown in Fig. S22 in the SI.) All PMMA films were annealed for 20 min at 90 °C. Finally, 20 nm of silver were evaporated through shadow masks onto the dielectric as semi-transparent top electrodes. (For the capacitors, the area of electrode overlap A is 1 mm^2.) All thin-film samples and devices were illuminated using a Dymax ECE 2000 flood lamp (13 mW cm^{-2} at 320 to 390 nm) and the dose was monitored using a Dymax Accu-Cal 50 UV dose meter. A fixed UV dose (as measured by the dose meter) of 5 J cm^{-2} was applied in all experiments. Thermal switching (from VHF to DHA) was carried out on a hot plate at 90 °C for 5 min. If not indicated otherwise all fabrication steps from deposition of the bottom electrodes to characterization and illumination/annealing were carried out in a nitrogen-filled glovebox.

Transistor characterization

The polymer transistors were characterized in the dark, in a nitrogen-filled glovebox using a Keithley 4200-SCS parameter analyzer. Transistor figures of merit, *i.e.* field-effect mobility and threshold voltage were derived from transfer characteristics following procedures described in the literature.[29] The V_{GS} fitting range for determining the threshold voltage was chosen from −20 to −50 V. Constant bias stress was applied for 2 h (cumulative) between drain and source electrodes (V_{DS} = −50 V) and gate and source electrodes (V_{GS} = −50 V).[30] During this time the bias stress was only paused to record transfer characteristics.

Impedance spectroscopy and impedance data analysis

Impedance spectra were recorded in the dark under ambient conditions using a Novocontrol Alpha-A impedance analyzer with a ZG4 test interface and measurements were carried out in air by applying an AC voltage of 1 V rms and sweeping the angular frequency from 10^6 to 1 Hz (35 data points with equal logarithmic spacing, no DC off-set). EISSA (electrochemical impedance spectroscopy spectrum analyzer) software was used for fitting of the impedance data. The details of the fitting procedure, equations and further information on the impedance formalism that was adapted in this study can be found in the SI section S3.

Results and discussion

Photo switchable capacitors

Three different derivatives of DHA/VHF molecular switches were blended with PMMA in order to fabricate light switchable capacitors (MIM, metal–insulator–metal devices). Fig. S1 shows the molecular structures of the switches, namely DHA/VHF-Ph, DHA/VHF-OMe and DHA/VHF-F_2. Ionization potentials, electron affinities and dipole moments of these materials are summarized in Table S1. The isomerization from DHA to VHF was induced by exposure to UV light, while the backreaction from VHF to DHA was achieved *via* thermal annealing at 90 °C for 5 min. Fig. 2a clearly depicts the typical color change from pale yellow (DHA) to orange/red (VHF), indicating that the isomerization reaction readily occurs in the PMMA matrix. For the capacitor and transistor devices 20 nm of silver were used as semi-transparent top electrodes, allowing for high UV light transparency (see Fig. S2). This switching is also evident in the obtained impedance data: In order to study the switching of the DHA/VHF molecules in the PMMA matrix, capacitors were subjected to eight switching cycles, where one cycle consists of a UV exposure step (DHA to VHF) and one thermal annealing step (VHF to DHA). After each UV and each annealing step, the impedance spectrum was measured. Fig. 2b–d depicts the data as Nyquist plot (Z'' *vs.* Z') as well as Bode plot ($|Z^*|$ *vs.* f and phase angle φ *vs.* f) for eight cycles of switching for a PMMA:DHA/VHF-Ph blend capacitor.

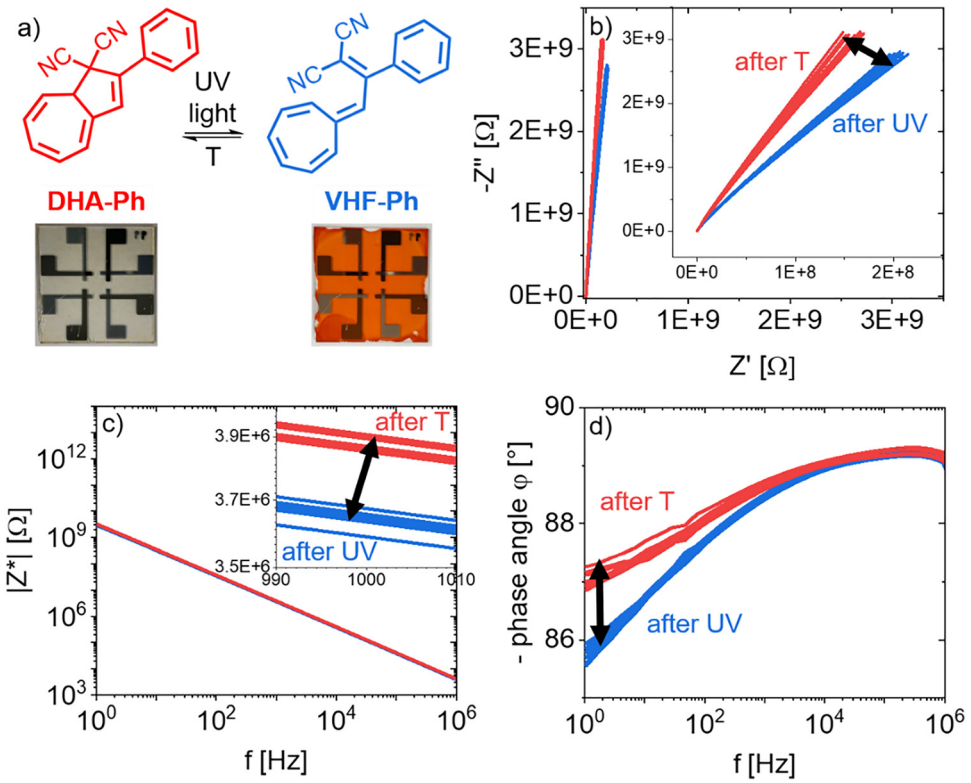

Fig. 2 Stimuli-responsive capacitors enabled by PMMA blends with DHA/VHF-Ph photo-/thermochromic molecules. (a) Molecular structure of both isomers of the molecular switch and photographs of a substrate with four capacitor devices after thermal annealing (left, switch in DHA form) and after UV light exposure (right, switch in VHF form). (b)–(d) Nyquist and Bode plot of impedance data collected for eight switching cycles. Traces in red correspond to data measured after annealing and traces in blue correspond to data measured after UV exposure. (The Nyquist plot in panel b) is shown on orthonormal axes, while its inset is not. Note that phase angles of capacitors are negative per definition, which describes the scenario that the current is leading the voltage.

The corresponding data for PMMA:DHA/VHF-OMe blend, PMMA:DHA/VHF-F_2 blend and a reference capacitor without any photoswitch can be found in Fig. S3.

Based on these data, the frequency-dependent complex dielectric permittivity ε_r^* was evaluated by calculating its real part ε_r' and imaginary part ε_r'' (for every frequency) using eqn (1) to (3), with the thickness of the dielectric d, vacuum permittivity ε_0 and area of electrode overlap A (= 1 mm^2). ε_r' and ε_r'' are sometimes referred to as dielectric permittivity and dielectric loss respectively.[23] Further information on this impedance formalism is given in the SI section S3.

$$\varepsilon_r' = \frac{d}{\omega\varepsilon_0 A}\frac{-Z''}{(Z'^2+Z''^2)} \quad (1)$$

$$\varepsilon_r'' = \frac{d}{\omega\varepsilon_0 A}\frac{Z'}{(Z'^2+Z''^2)} \quad (2)$$

$$|\varepsilon_r^*| = \sqrt{\varepsilon_r'^2+\varepsilon_r''^2} \quad (3)$$

Fig. 3a and b show that both, the real and imaginary part of the permittivity increase after UV exposure. The increase in the imaginary part is more pronounced at lower frequencies. Furthermore, the modulus of the complex permittivity $|\varepsilon_r^*|$ and the loss tangent tan (δ) were calculated (see Fig. S4). In absolute values, $|\varepsilon_r^*|$ switches between around 3.56 and 3.96 (at f = 1 Hz), which corresponds to a switching of capacitance (per unit area) between 4.9 and 5.4 nF cm^{-2}. The frequency-independent increase in ε_r' upon UV irradiation is related to the increased dipole moment of VHF in comparison to DHA (see Table S1) resulting in a larger polarizability of the blend. Furthermore, Fig. 2 indicates a slight decrease in resistance after UV irradiation, which is consistent with an increase in dielectric loss and in agreement with increased single molecule conductance of VHF correlated with the reduced HOMO–LUMO gap.[8,31] The switching in ε_r'' at low frequencies could also stem from switch molecules affecting the relaxation of the PMMA side groups. It has been reported that the relaxation of the carboxymethyl (–$COOCH_3$) side groups (β relaxation mode) results in a peak in the ε_r'' spectrum between 1 and 10 Hz,[18] which is in good agreement with our results (see Fig. S5). However, in the blend system with DHA/VHF this relaxation peak cannot be observed, possibly due to the fact that the presence of the switches hinders the movement of the polymer side groups, with this effect being stronger for DHA compared to VHF. Our results show that the contribution of ε_r' (related to the changing dipole moment of DHA/VHF) dominates the strong increase in $|\varepsilon_r^*|$ (and therefore capacitance) after UV illumination. Similar results

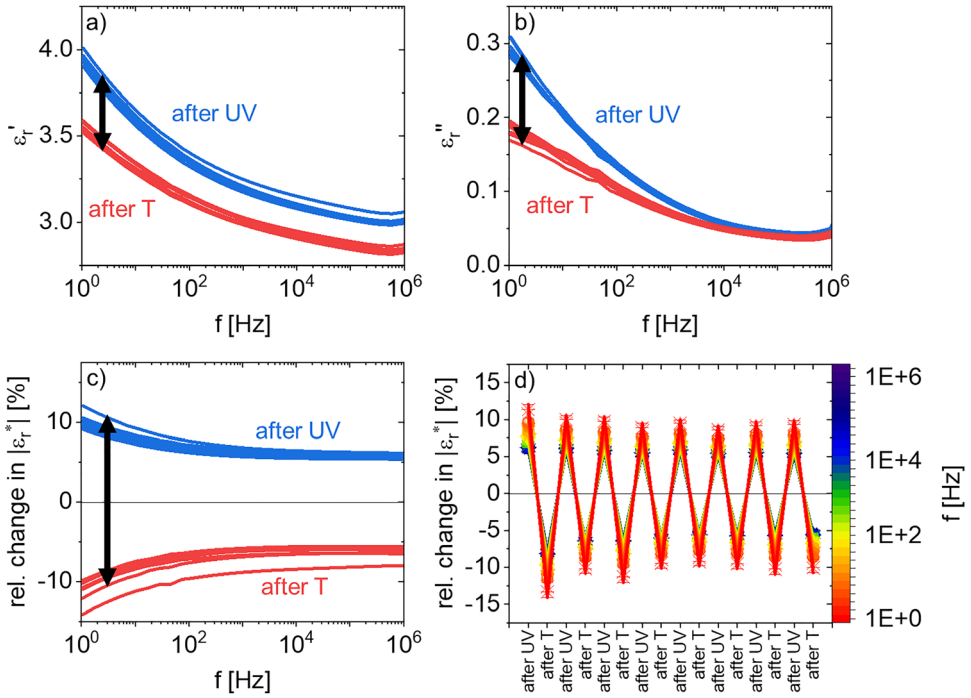

Fig. 3 Analysis of the frequency-dependent complex permittivity ε_r^*. (a) and (b) Real and imaginary part of ε_r^*. (c) Relative change in the modulus of the complex permittivity (from one processing step to the next) as a function of frequency. Traces in red correspond to data measured after annealing and traces in blue correspond to data measured after UV exposure. (d) Relative change in the modulus of the complex permittivity over the course of eight switching cycles. The color coding from red to dark blue corresponds to the frequency at which the permittivity was evaluated. (Note that panels (c) and (d) represent the same data in two different ways.)

were reported for PMMA-based capacitors containing azobenzene[21] and spiropyran.[22] Fig. 3c and d show the relative changes of $|\varepsilon_r^*|$ (from one processing step to the next) as a function of frequency and after each individual step. These results indicate that the modulus of the permittivity increases as a result of UV exposure (consistent with the increasing dipole moment, see Table S1[32]), while it decreases after thermal annealing. Furthermore, the changes are more pronounced at lower frequencies (due to the contribution of ε_r'') and no apparent cycling fatigue (reduction in magnitude of switching) can be observed.

An alternative approach for evaluating impedance spectra is to fit the data to an equivalent circuit model in order to better understand the physical and chemical processes, which are possibly occurring during the experiment. For example, Rampi *et al.* reported that alkanethiol self-assembled monolayers between two opposing mercury surfaces can be modelled with an RC element (*i.e.* resistor and capacitor in parallel).[33] Jin *et al.* used a more complicated circuit of a resistor in series with two RC elements to describe the electrochemical processes in electrochromic displays.[34] The molecules reported in that study contain photochromic diarylethene units, but their ability to photoisomerize was not investigated with impedance spectroscopy. To the best of our knowledge, there are no reports in the literature, which describe and quantify the switching of photochromic molecules using equivalent circuit analysis. We here employ such a procedure, which in particular allows to extract dielectric permittivities from the frequency-dependent impedance data. The details are given in the SI.

Here, an RC element model is chosen yielding the fitted resistance R and the fitted capacitance C (which can be converted to the area-normalized capacitance C_i). A representative fit of data measured on PMMA:DHA/VHF-Ph-based MIM devices is given in Fig. 4c. (Results obtained with different equivalent circuit models as well as details on the fitting procedure are given in the SI) Fig. 4a and b show that both circuit parameters of the RC model switch reversibly over the course of eight UV/T cycles. With the fitted capacitance it is possible to calculate the permittivity ε_r of the sample using eqn 4. Furthermore, we conclude that approach of describing the sample as a capacitor is an approximation justified by the large values of resistance (in the GΩ range).

$$\varepsilon_r = \frac{C_{\text{fitted}} d}{\varepsilon_0 A} \tag{4}$$

Furthermore, a comparison of the permittivities derived from the RC element model with the results obtained by directly analyzing the complex impedance data (at f = 1 Hz) shows that both approaches yield comparable results (see Fig. 4d), underlining the validity of the fitting approach.

Fig. 4 shows the switching in permittivity for PMMA blends containing three different DHA/VHF derivatives obtained *via* fitting with a RC element model. The largest change in permittivity is observed for blends with the unsubstituted derivative DHA/VHF-Ph, while the lowest change is observed for the fluorinated derivative DHA/VHF-F_2. This trend is in agreement

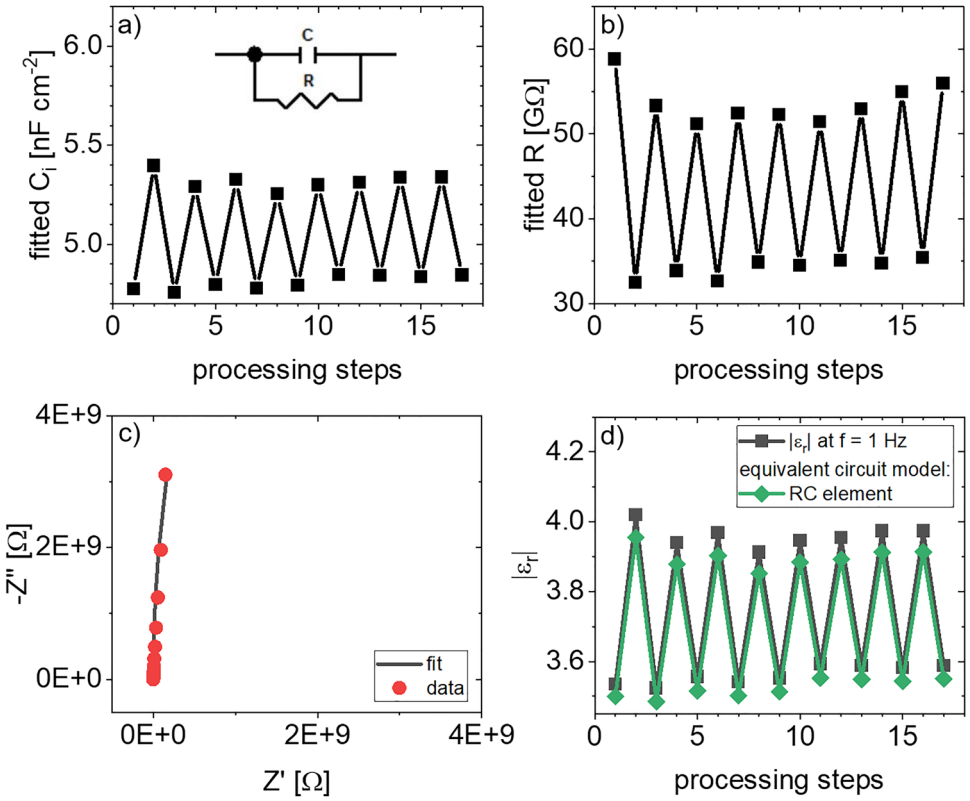

Fig. 4 Equivalent circuit fitting analysis using an RC element model of impedance data from a PMMA:DHA/VHF-Ph MIM devices acquired over the course of eight UV/T cycles. Fitted circuit element parameters: (a) Area-normalized capacitance, (b) resistance. (c) Fitted (representative) Nyquist plot on orthonormal axes. (d) Resulting permittivities from the equivalent circuit (green diamonds) compared to permittivities from the complex frequency-dependent impedance at f = 1 Hz.

with the expectation based on the calculated dipole moments of the switches (see Table S1). The differences in dipole moment of the isomers were determined as 4.95 D for DHA/VHF-Ph, 4.42 D for DHA/VHF-OMe and 4.22 D for DHA/VHF-F_2. Fig. S14 indicates that the same qualitative trend is obtained when other equivalent circuit models are used. All isomers demonstrate a very good switching stability over multiple cycles (Fig. 5).

UV/Vis absorption

To study the cycling fatigue, PMMA blends with DHA/VHF switches were investigated using UV/Vis absorption spectroscopy. Spectra were recorded on pristine films and after the first UV light irradiation in order to determine the characteristic absorption bands of the DHA and VHF isomers. In agreement with the literature[35] the DHA isomers showed a maximum absorption around 360 to 370 nm, while the VHF isomers absorbed around

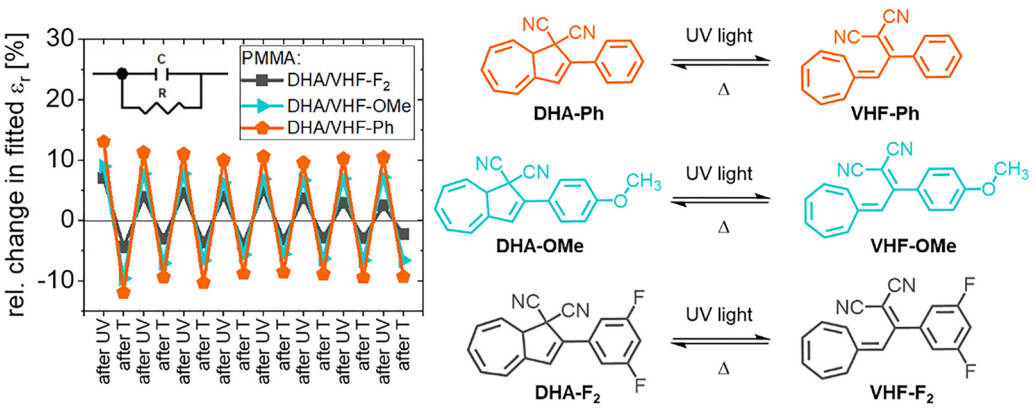

Fig. 5 Comparing the switching in permittivity for PMMA:DHA/VHF capacitors containing three different DHA/VHF derivatives (DHA/VHF-Ph, DHA/VHF-OMe, DHA/VHF-F_2). The relative change in permittivity was determined by fitting an RC element model to impedance data collected over the course of eight UV/T cycles.

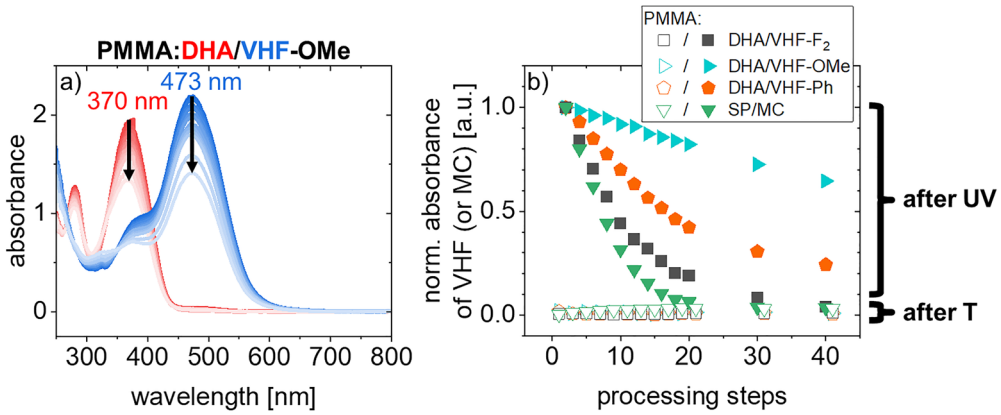

Fig. 6 (a) UV/Vis absorption spectra of (a) PMMA:DHA/VHF-OMe blend films measured over 20 UV/T cycles. Blue traces: measured after UV light exposure (5 J cm^{-2}). Red traces: measured after thermal annealing (90 °C for 5 min). (b) Comparing cycling fatigue behavior of PMMA:DHA/VHF-OMe, PMMA:DHA/VHF-Ph, PMMA:DHA/VHF-F_2 and PMMA:SP/MC (spiropyran/merocyanine) blend films using UV/Vis absorption spectroscopy. The graph displays the normalized absorption (measured at wavelength of maximum absorption) of VHF around 470 to 480 nm and MC around 570 nm (respectively). Empty symbols indicate that the switch is in its DHA (or SP) form.

470 to 485 nm. Additionally, the switching fatigue of the blend films was studied over the course of 20 UV/T cycles (*i.e.* 20 UV and 20 annealing steps). All recorded spectra are shown in Fig. 6a and Fig. S15. The absorbance of the VHF isomer at λ_{max} was used as an indicator of switching fatigue (see SI for experimental details). Fig. 6b demonstrates that DHA/VHF-OMe shows remarkable switching stability. After 20 UV/T cycles the VHF absorption has only decreased by 35%. Furthermore, all three DHA/VHF derivatives and especially DHA/VHF-OMe show superior fatigue resistance compared to the well-known spiropyran switch, which degrades almost completely within the first 10 cycles. Possibly, the DHA/VHF switches are less prone to photo-oxidation, since they exhibit higher ionization potentials than SP/MC switches (see Table S1). Such photo-oxidation can occur as a result of the repeated UV light exposure and is known to be a major degradation path in spiropyran systems.[36,37] Other reports indicate that spiropyrans tend to aggregate due to the presence of ionic moieties in the merocyanine form.[38–40] Neither DHA nor VHF isomers contain ionic moieties, which presumably is another reason for the improved fatigue resistance.

Photoswitchable transistors

The first successful application of insulating polymer:photoswitch blends as gate dielectrics in OFETs was reported by Shen *et al.*[41] The authors blended spiropyran molecules into PMMA and observed an increase in capacitance due to photoisomerization of the low dipole moment spiropyran to the high dipole moment merocyanine. Increased drain current in transistors was ascribed to the increase in dielectric permittivity. Lee *et al.* used blends of PMMA and azobenzene switches to construct UV sensors and also concluded that isomerization to the high dipole moment isomer of the photoswitch increases the capacitance of the dielectric blend which in turn leads to higher drain current in transistors.[42] Here, this concept of light-switchable gate dielectrics is extended for the first time to blends with DHA/VHF molecular switches. PMMA:DHA/VHF blends were applied as gate dielectrics in P3HT OFETs and device characteristics were recorded over the course of eight UV/T cycles. The resulting transfer and output characteristics for transistors with PMMA:DHA/VHF blend and unblended PMMA (as reference) dielectrics are summarized in Fig. 7 and Fig. S16, S17. Fig. 7a shows that the obtained transfer characteristics for transistors with PMMA:DHA/VHF-OMe blend dielectric after UV and after thermal annealing can be clearly distinguished. In contrast to previous reports employing PMMA:SP/MC blends,[43,44] these characteristics show only negligible hysteresis regardless of the state of the switch. UV exposure leads to an increase in drain current caused by a shift of the threshold voltage (of around 15 V) towards more positive gate-source bias. Furthermore, the modulation of the transfer characteristics can be related to a change in field-effect mobility as indicated in Fig. 7b. Similar behavior was observed for the blends with DHA/VHF-Ph and DHA/VHF-F_2 (see Fig. S16). A quantitative comparison of the stimuli-modulated field-effect mobility (determined at maximum negative gate bias) for blends with three different derivatives of the switch is given in Fig. 7c. The area-normalized capacitances of the gate dielectrics that were used to calculate the mobilities, are summarized in Table S2. These values were calculated by using the dielectric permittivities obtained by fitting impedance data using a single capacitor as equivalent circuit (see SI for details). The reversible shifts of threshold voltage for all three blends are shown in Fig. S18 as well as further characterization including bias stress (Fig. S19) and long-term (Fig. S20) stability.

In our previous work we were able to show that stimuli-responsive organic transistors can be enabled by blending DHA/VHF molecular switches into the active channel (semiconductor) of the device.[32] A reversible tuning of transfer characteristics was observed upon alternating UV light irradiation and thermal annealing. Increased on-current and a shift of threshold voltage towards more positive gate-source bias as a consequence of UV irradiation suggested that the VHF isomer

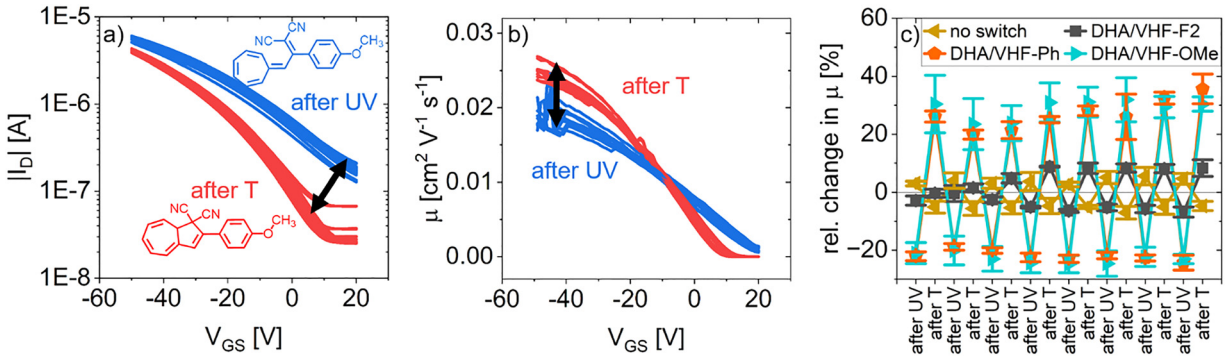

Fig. 7 Stimuli-responsive organic transistors enabled by using PMMA blends with DHA/VHF photo-/thermochromic molecules as gate dielectrics. (a) Reversible changes of transfer characteristics in a transistor with PMMA:DHA/VHF-OMe dielectric induced by UV light illumination (blue lines) and thermal annealing (red lines) for eight UV/T cycles (V_{DS} = −50 V). (b) Gate-source bias-dependent field-effect mobilities. (c) Reversible change in mobility (at V_{GS} = −50 V) for blends containing three different DHA/VHF derivatives (PMMA:DHA/VHF-OMe, PMMA:DHA/VHF-Ph, PMMA:DHA/VHF-F_2) and a reference device without any switch. (The error bars represent the standard deviation of at least three devices.)

can act as a dopant, which is activated with light. Here, we report similar observations, when incorporating DHA/VHF photoswitches into the gate dielectric, rather than the active layer. Due to the spatial separation of the switch and the semiconductor, it seems unlikely that a doping-like mechanism can occur. Hence, other effects such as a change in gate dielectric capacitance (which was observed experimentally, see above) or energetic disorder should be considered. As discussed in the previous section, the isomerization from DHA to VHF increases the dielectric permittivity of PMMA:DHA/VHF blends and therefore yields an increase of the capacitance of the gate dielectric of the transistor. This should be expected to lead to higher drain currents, but should either not affect the threshold voltage or rather lead to more negative threshold voltages.[45] Veres *et al.* reported that energetic disorder at the semiconductor-dielectric interface induced by large molecular dipoles within the dielectric leads to lower mobility and shifts the threshold voltage to more negative gate-source bias.[16] In our case, a transition from the low dipole moment DHA to the high dipole moment VHF leads to a decrease in mobility and a threshold voltage shift to more positive gate-source bias. Therefore, the changing capacitance and the energetic disorder both fail to fully explain our results and a more complicated mechanism or two effects simultaneously seem to be at place. Potential explanations include (1) interfacial mixing between the PMMA:photoswitch blend and the semiconductor and/or (2) phase separation between PMMA and the photoswitch which brings the latter in direct contact with the semiconductor. Both scenarios could potentially cause doping effects through the strong electron accepting properties of VHF,[46] similar to when the switch is blended directly into the semiconductor. Alternatively, the formation of photoswitch aggregates with at least partially aligned dipole moments and the resulting built-in electric field would also cause threshold voltage shifts towards more positive threshold voltages, as observed for OFETs employing well-ordered SAM-based interfacial dipoles.[14,47–49] In order to clarify the exact mechanism at place, further experimental studies carefully examining the microstructure of the interface will be necessary.

Conclusion

In the first part of this study, capacitors were fabricated by blending the insulating polymer PMMA with DHA/VHF photo-/thermochromic molecules. The reversible isomerization of the molecular switches can be observed in capacitors (MIM, metal–insulator–metal devices) and is studied in detail by using impedance spectroscopy. In order to quantify the reversible switching of the system, the resulting impedance data is analyzed by following two different approaches: (1) calculating the frequency-dependent complex dielectric permittivity from the real and the imaginary part of the complex impedance for every frequency and (2) determination of the dielectric permittivity through equivalent circuit fitting of the complex impedance data. To the best of our knowledge, this is the first time that an equivalent circuit fitting methodology is applied to investigate the photoisomerization of molecular switches. In addition to the switching of the capacitance/permittivity, the fit of an RC-element captures a slight switching of a resistive component which correlates well with previous reports on switching of single molecule conductance. This study underlines that impedance spectroscopy is a straightforward tool to capture and accurately quantify the reversible switching of photochromic molecules in stimuli-responsive organic electronic devices.

Furthermore, the PMMA:DHA/VHF blends are successfully applied to construct light- and temperature-responsive organic transistors. We show that the transistor characteristics can be tuned reversibly *via* the isomerization of DHA/VHF molecular switches within the gate dielectric. The charge carrier mobility in particular is modulated by around 20–30% by applying subsequent UV light and thermal annealing treatments. Finally, the superior resistance to switching fatigue compared to the known spiropyran switch is demonstrated. It can be concluded that DHA/VHF molecular switches and the reported reversibly switchable transistors open up new opportunities for next-generation stimuli-responsive organic electronic devices and memory applications.

Conflicts of interest

There are no conflicts to declare.

Data availability

The data supporting this article are shown in the supplementary information (SI). Supplementary information is available. See DOI: https://doi.org/10.1039/d5tc01677k.

The raw data is available from the authors upon request.

Acknowledgements

The authors thank C. Bauer, M. Beuchel, F. Keller, S. Koynova and V. Maus for the technical support. This work was partially funded by the German Research Foundation (DFG) under Grant 551494522 and by the Max Planck Society. FL thanks the Ingeborg-Gross foundation. Open Access funding provided by the Max Planck Society.

References

1 U. Kraft, T. Zaki, F. Letzkus, J. N. Burghartz, E. Weber, B. Murmann and H. Klauk, *Adv. Electron. Mater.*, 2019, **5**, 1800453.
2 S. Lee, S. Kim and H. Yoo, *Polymers*, 2021, **13**, 3774.
3 Y. Wakayama, R. Hayakawa and H.-S. Seo, *Sci. Technol. Adv. Mater.*, 2014, **15**, 024202.
4 J. Milvich, T. Zaki, M. Aghamohammadi, R. Rödel, U. Kraft, H. Klauk and J. N. Burghartz, *Org. Electron.*, 2015, **20**, 63–68.
5 Y. Ishiguro, R. Hayakawa, T. Chikyow and Y. Wakayama, *J. Mater. Chem. C*, 2013, **1**, 3012–3016.
6 Y. Ishiguro, R. Hayakawa, T. Yasuda, T. Chikyow and Y. Wakayama, *ACS Appl. Mater. Interfaces*, 2013, **5**, 9726–9731.
7 Y. Ishiguro, R. Hayakawa, T. Chikyow and Y. Wakayama, *ACS Appl. Mater. Interfaces*, 2014, **6**, 10415–10420.
8 S. Lara-Avila, A. V. Danilov, S. E. Kubatkin, S. L. Broman, C. R. Parker and M. B. Nielsen, *J. Phys. Chem. C*, 2011, **115**, 18372–18377.
9 S. L. Broman, S. Lara-Avila, C. L. Thisted, A. D. Bond, S. Kubatkin, A. Danilov and M. B. Nielsen, *Adv. Funct. Mater.*, 2012, **22**, 4249–4258.
10 C. Huang, M. Jevric, A. Borges, S. T. Olsen, J. M. Hamill, J.-T. Zheng, Y. Yang, A. Rudnev, M. Baghernejad, P. Broekmann, A. U. Petersen, T. Wandlowski, K. V. Mikkelsen, G. C. Solomon, M. Brøndsted Nielsen and W. Hong, *Nat. Commun.*, 2017, **8**, 15436.
11 T. Li, M. Jevric, J. R. Hauptmann, R. Hviid, Z. Wei, R. Wang, N. E. A. Reeler, E. Thyrhaug, S. Petersen, J. A. S. Meyer, N. Bovet, T. Vosch, J. Nygård, X. Qiu, W. Hu, Y. Liu, G. C. Solomon, H. G. Kjaergaard, T. Bjørnholm, M. B. Nielsen, B. W. Laursen and K. Nørgaard, *Adv. Mater.*, 2013, **25**, 4164–4170.
12 Y. Wang, X. Huang, T. Li, L. Li, X. Guo and P. Jiang, *Chem. Mater.*, 2019, **31**, 2212–2240.
13 R. P. Ortiz, A. Facchetti and T. J. Marks, *Chem. Rev.*, 2010, **110**, 205–239.
14 U. Kraft, U. Zschieschang, F. Ante, D. Kälblein, C. Kamella, K. Amsharov, M. Jansen, K. Kern, E. Weber and H. Klauk, *J. Mater. Chem.*, 2010, **20**, 6416–6418.
15 U. Kraft, M. Sejfić, M. J. Kang, K. Takimiya, T. Zaki, F. Letzkus, J. N. Burghartz, E. Weber and H. Klauk, *Adv. Mater.*, 2015, **27**, 207–214.
16 J. Veres, S. D. Ogier, S. W. Leeming, D. C. Cupertino and S. Mohialdin Khaffaf, *Adv. Funct. Mater.*, 2003, **13**, 199–204.
17 T. Richards, M. Bird and H. Sirringhaus, *J. Chem. Phys.*, 2008, **128**, 234905.
18 I. M. Kalogeras, E. R. Neagu and A. Vassilikou-Dova, *Macromolecules*, 2004, **37**, 1042–1053.
19 W. Shi, C. Fang, Q. Pan, X. Sun, Q. Gu, D. Xu and J. Yu, *React. Funct. Polym.*, 2000, **44**, 177–182.
20 D. Lei, J. Runt, A. Safari and R. E. Newnham, *Macromolecules*, 1987, **20**, 1797–1801.
21 V. Zaporojtchenko, C. Pakula, S. W. Basuki, T. Strunskus, D. Zargarani, R. Herges and F. Faupel, *Appl. Phys. A*, 2011, **102**, 421–427.
22 M. Gagliardi, F. Pignatelli and V. Mattoli, *Sens. Actuators, A*, 2020, **302**, 111804.
23 D. Luo and L. Deng, *Appl. Phys. Lett.*, 2006, **88**, 181104.
24 J. T. S. Irvine, D. C. Sinclair and A. R. West, *Adv. Mater.*, 1990, **2**, 132–138.
25 R. R. Gaddam, L. Katzenmeier, X. Lamprecht and A. S. Bandarenka, *Phys. Chem. Chem. Phys.*, 2021, **23**, 12926–12944.
26 E. P. Randviir and C. E. Banks, *Anal. Methods*, 2022, **14**, 4602–4624.
27 K. H. Au-Yeung, T. Kühne, O. Aiboudi, S. Sarkar, O. Guskova, D. A. Ryndyk, T. Heine, F. Lissel and F. Moresco, *Nanoscale Adv.*, 2022, **4**, 4351–4357.
28 U. Kraft, M. Nikolka, G. J. N. Wang, Y. Kim, R. Pfattner, M. Alsufyani, I. McCulloch, B. Murmann and Z. Bao, *J. Phys. Mater.*, 2023, **6**, 025001.
29 Z. A. Lamport, H. F. Haneef, S. Anand, M. Waldrip and O. D. Jurchescu, *J. Appl. Phys.*, 2018, **124**, 071101.
30 M. Nguyen, U. Kraft, W. L. Tan, I. Dobryden, K. Broch, W. Zhang, H.-I. Un, D. Simatos, D. Venkateshavaran, I. McCulloch, P. M. Claesson, C. R. McNeill and H. Sirringhaus, *Adv. Mater.*, 2023, **35**, 2205377.
31 S. L. Broman and M. B. Nielsen, *Phys. Chem. Chem. Phys.*, 2014, **16**, 21172–21182.
32 S. Gebel, O. Aiboudi, V. Grigorescu, Z. Ling, T. Marszalek, P. W. M. Blom, C. Ramanan, F. Lissel and U. Kraft, *Adv. Electron. Mater.*, 2024, 2400455, DOI: 10.1002/aelm.202400455.
33 M. A. Rampi, O. J. A. Schueller and G. M. Whitesides, *Appl. Phys. Lett.*, 1998, **72**, 1781–1783.
34 H. Jin, J. Tian, S. Wang, T. Tan, Y. Xiao and X. Li, *RSC Adv.*, 2014, **4**, 16839–16848.

35 H. Torres-Pierna, C. Roscini, A. Vlasceanu, S. L. Broman, M. Jevric, M. Cacciarini and M. B. Nielsen, *Dyes Pigm.*, 2017, **145**, 359–364.
36 X. Li, Y. Wang, T. Matsuura and J. Meng, Molecular Crystals and Liquid Crystals Science and Technology. Section A, *Mol. Cryst. Liq. Cryst.*, 2000, **344**, 301–306.
37 T. Yoshida and A. Morinaka, *J. Photochem. Photobiol., A*, 1992, **63**, 227–234.
38 A. Radu, R. Byrne, N. Alhashimy, M. Fusaro, S. Scarmagnani and D. Diamond, *J. Photochem. Photobiol., A*, 2009, **206**, 109–115.
39 R. Matsushima, M. Nishiyama and M. Doi, *J. Photochem. Photobiol., A*, 2001, **139**, 63–69.
40 S. Abe, Y. Nishimura, I. Yamazaki and N. Ohta, *Chem. Lett.*, 1999, 165–166.
41 Q. Shen, L. Wang, S. Liu, Y. Cao, L. Gan, X. Guo, M. L. Steigerwald, Z. Shuai, Z. Liu and C. Nuckolls, *Adv. Mater.*, 2010, **22**, 3282–3287.
42 K. E. Lee, J. U. Lee, D. G. Seong, M.-K. Um and W. Lee, *J. Phys. Chem. C*, 2016, **120**, 23172–23179.
43 P. Lutsyk, K. Janus, J. Sworakowski, G. Generali, R. Capelli and M. Muccini, *J. Phys. Chem. C*, 2011, **115**, 3106–3114.
44 M. Brohmann, S. Wieland, S. Angstenberger, N. J. Herrmann, J. Lüttgens, D. Fazzi and J. Zaumseil, *ACS Appl. Mater. Interfaces*, 2020, **12**, 28392–28403.
45 M. Aghamohammadi, R. Rödel, U. Zschieschang, C. Ocal, H. Boschker, R. T. Weitz, E. Barrena and H. Klauk, *ACS Appl. Mater. Interfaces*, 2015, **7**, 22775–22785.
46 L. Gobbi, P. Seiler, F. Diederich, V. Gramlich, C. Boudon, J.-P. Gisselbrecht and M. Gross, *Helv. Chim. Acta*, 2001, **84**, 743–777.
47 K. P. Pernstich, S. Haas, D. Oberhoff, C. Goldmann, D. J. Gundlach, B. Batlogg, A. N. Rashid and G. Schitter, *J. Appl. Phys.*, 2004, **96**, 6431–6438.
48 S. Kobayashi, T. Nishikawa, T. Takenobu, S. Mori, T. Shimoda, T. Mitani, H. Shimotani, N. Yoshimoto, S. Ogawa and Y. Iwasa, *Nat. Mater.*, 2004, **3**, 317–322.
49 U. Zschieschang, F. Ante, M. Schlörholz, M. Schmidt, K. Kern and H. Klauk, *Adv. Mater.*, 2010, **22**, 4489–4493.

